Journal of Hepatocellular Carcinoma

Dovepress
Taylor & Francis Group

Open Access Full Text Article

ORIGINAL RESEARCH

CT-Based Radiomics Features Combined with AFP for Predicting Vessels Encapsulating Tumor Clusters and Prognosis of Hepatocellular Carcinoma

Yunyun Wei[1,2,*], Shiyuan Huang[3,*], Luyu Huang[4,*], Wei Pei[1,2], Yang Zuo[1,2], Hai Liao[1,2]

[1]Department of Medical Imaging Center, Guangxi Medical University Cancer Hospital, Nanning, Guangxi, People's Republic of China; [2]Guangxi Key Clinical Specialty Department (Medical imaging Department), Guangxi Medical University Cancer Hospital, Nanning, Guangxi, People's Republic of China; [3]Hospital Administrative Department, The People's Hospital of Guangxi Zhuang Autonomous Region, Nanning, Guangxi, People's Republic of China; [4]Department of Pathology, Guangxi Medical University Cancer Hospital, Nanning, Guangxi, People's Republic of China

*These authors contributed equally to this work

Correspondence: Hai Liao, Department of Medical Imaging Center, Guangxi Medical University Cancer Hospital, Nanning, Guangxi, People's Republic of China; Guangxi Key Clinical Specialty Department (Medical imaging Department), Guangxi Medical University Cancer Hospital, Nanning, Guangxi, People's Republic of China, Tel +86-771-5334951, Email 42442427@qq.com

Objective: This study aims to develop a CT-based radiomics nomogram for preoperative prediction of vessels encapsulating tumor clusters (VETC) and patient prognosis in hepatocellular carcinoma (HCC).

Patients and Methods: The retrospective, single-center study included 231 (77 VETC+ and 154 VETC-) HCC patients who underwent preoperative CT scan, and were randomly divided into training and validation cohorts at a 7:3 ratio. Radiomics features were extracted from CT images during the plain, arterial and venous phases. These features were then selected using the Least Absolute Shrinkage and Selection Operator (LASSO). Predictive factors were chosen through univariate and multivariate logistic regression. A prognostic nomogram integrating clinical factor and radiomics features was developed and validated. The model's predictive accuracy was systematically evaluated using the area under the receiver operating characteristic curve (AUC), while calibration curves assessed agreement between predicted and observed outcomes. To quantify clinical utility, decision curve analysis (DCA) was implemented. Furthermore, the model's prognostic performance for postoperative disease-free survival (DFS) was examined through Kaplan-Meier analysis.

Results: The nomogram integrating four radiomics features and alpha-fetoprotein (AFP) exhibited robust predictive performance, with AUC values of 0.782 (95% confidence interval [CI]: 0.708–0.856) in the training cohort and 0.755 (95% CI: 0.628–0.882) in the validation cohort. Calibration curves demonstrated excellent agreement between predicted and observed outcomes in both cohorts. DCA revealed significant clinical utility of the nomogram. Additionally, the model-stratified VETC+ HCC patients showed significantly worse DFS compared to VETC- counterparts (log-rank p = 0.035).

Conclusion: The CT-based radiomics nomogram, integrating radiomics features and AFP, provides a non-invasive and reliable tool for predicting VETC and stratifying prognosis in HCC patients.

Keywords: hepatocellular carcinoma, radiomics, computed tomography, vessels encapsulating tumor clusters, prognosis

Introduction

Hepatocellular carcinoma (HCC) stands as the sixth most prevalent cancer globally and ranks third among the primary causes of cancer-related fatalities.[1] While surgical resection provides a viable curative method, the recurrence rate within five years can reach up to 70%,[2] considerably affecting long-term survival.

The invasion and metastasis of HCC, a highly vascular solid tumor, are intimately tied to abnormal angiogenesis.[3,4] Among its manifestations, microvascular invasion (MVI), facilitated by epithelial-mesenchymal transition (EMT),[5] is

Received: 22 May 2025
Accepted: 9 September 2025
Published: 13 September 2025

a known predictor of postoperative recurrence.[6] Nevertheless, even patients without MVI face a considerable risk of recurrence,[7,8] highlighting the necessity to investigate additional prognostic markers. Fang et al[9] uncovered vessels encapsulating tumor clusters (VETC) as a distinct vascular metastasis pattern independent of EMT, in which tumor clusters enter blood vessels directly via $CD34^{+}$ endothelium. The VETC pattern is strongly correlated with early recurrence and poor prognosis in HCC.[10,11] Notably, VETC is observed in approximately 20–30% of patients undergoing HCC resection.[10–12] The 5-year overall survival rate and disease-free survival rate of VETC+ HCC patients are significantly lower than those of VETC- patients (42.2% vs 74.6% and 25.7% vs 56.8%, respectively).[12] Moreover, scholars found that VETC may act as a predictor of sorafenib benefit for HCC. Sorafenib is effective in prolonging the survival of VETC+, but not VETC- HCC patients.[13] This indicates that VETC status not only informs prognosis but can also guide targeted therapy selection for HCC patients. However, the current diagnosis of VETC mainly relies on postoperative histopathological examination, resulting in a significant clinical application lag.

Radiomics, proposed by Lambin in 2012, converts medical images into mineable high-dimensional data by high-throughput extraction of quantitative features.[14] This approach has found broad application in diagnosing, evaluating treatment responses, and assessing prognosis in patients with HCC, showing notable efficacy.[15–17] This includes its application in predicting critical pathological features such as VETC, for which most existing studies have utilized MRI or ultrasound. In contrast, despite the pivotal role of CT in the standard clinical workflow of HCC, CT-based radiomics models remain underexplored.

Given the aforementioned background, we hypothesize that CT-based radiomics features may accurately predict VETC expression status and prognostic risk stratification in HCC patients. The CT-based radiomics nomogram constructed through multidimensional integration of radiomics features and clinical parameters is expected to overcome the spatiotemporal limitations of traditional pathological evaluation, providing critical decision support for precise diagnosis and treatment of HCC patients.

Materials and Methods

Patients

The protocol for this retrospective study was approved by the Ethics Committee of our hospital, and patient informed consent was waived. And this study was conducted in accordance with the Declaration of Helsinki.

Between December 2017 and May 2021, patients who underwent contrast-enhanced CT followed by curative hepatectomy were included. The inclusion criteria were as follows: (1) pathologically confirmed HCC with VETC results; (2) contrast-enhanced CT scan performed within one month before surgery; (3) CT images quality was adequate for analysis. The exclusion criteria were: (1) patients treated by cancer-related treatment preoperatively; (2) incomplete clinical laboratory data or pathology slides; (3) patients with other malignant tumors.

A total of 231 HCC patients (202 men and 29 women, mean age 52.9 years, range 24–81 years) were included in this study, consisting of 77 VETC+ and 154 VETC- patients. Patients were randomly assigned to the training cohort (n=162) and validation cohort (n=69) at a ratio of 7:3 using a random seed of 123. (Figure 1).

Pathological Evaluation

Two experienced pathologists, with 10 and 7 years of experience in pathological diagnosis respectively, independently evaluated all histopathological specimens. In cases of discordant conclusions, the specimens were submitted to a third pathologist and discussed until a consensus was reached. All pathologists were blinded to clinical, laboratory, imaging features, and follow-up data. Cases with visible VETC pattern in all or part of the HCC section were identified as VETC +, while those without any VETC patterns were identified as VETC-.[9]

CT Examination

CT scans were performed using a Siemens Sensation 64-slice spiral CT or a GE Discovery CT 750 HD spiral CT. The scanning parameters were set as follows: voltage of 120 kV, current of 230 mAs, matrix size of 512 x 512, field of view (FOV) ranging from 300 to 350 mm, pitch of 1, slice thickness of 5 mm, and slice interval of 5 mm. Iopromide injection

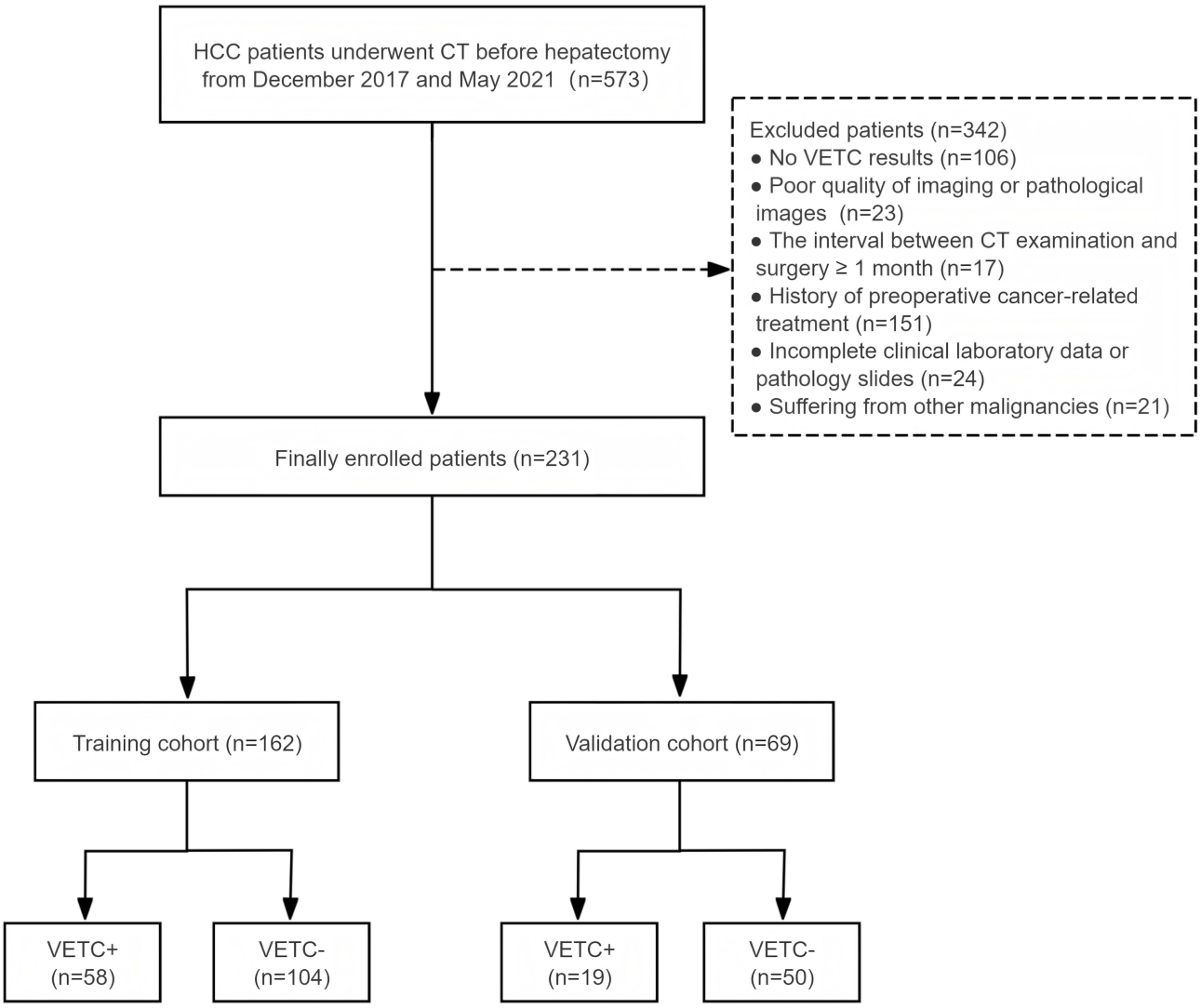

Figure 1 Flowchart of this study population.

(300 mg iodine /mL) was administered intravenously at a total volume calculated based on 1.5 mL/kg body weight. Dynamic contrast-enhanced scanning was performed with a bolus injection rate of 3 mL/s, and scans were acquired at 25s and 60s post-injection for the arterial and venous phases, respectively.

Clinical and Radiological Data Acquisition

Clinical data, including age; gender; body mass index (BMI); liver cirrhosis; alpha-fetoprotein (AFP; < 400 or ≥ 400 ng/mL); systemic immune inflammation index (SII); neutrophil-to-lymphocyte ratio (NLR; < 2 or ≥ 2); platelet-to-lymphocyte ratio (PLR; < 150 or ≥ 150); aspartate aminotransferase (AST) and alanine aminotransferase (ALT).

Imaging features were independently analyzed by two radiologists (H.L. and Y.W, with 16 and 7 years of experience in abdominal imaging, respectively) who were blinded to clinical, laboratory, histological and follow-up results. For discordant cases, the two radiologists met to discuss and draw final conclusions by consensus. Imaging features including tumor size, intratumoral necrosis, hepatic vein invasion, portal vein tumor thrombus, tumor capsule and tumor margin. Tumor size was defined as the maximum diameter of the tumor. Tumor margin were categorized as smooth (indicating an uninodular tumor), or irregular (indicating a focal or multinodular tumor).[18] Tumor capsule was classified as complete, incomplete or without tumor capsule. Complete tumor capsule was defined as complete peripheral rim of

hyperenhancement in the portal venous phase. Incomplete or without tumor capsule was defined as the absence or a disrupted "capsule" in any imaging plane.[19]

Follow-Up

Patients were followed up with AFP and imaging examinations every 3 to 6 months after hepatectomy. Tumor recurrence was determined using enhanced CT or MRI. Disease-free survival (DFS) was recorded, defined as the time from surgery to recurrence or death from any cause. For patients who were lost to follow-up, survival time was calculated from the date of surgery to the last follow-up.

Segmentation and Feature Extraction

Radiologist A (Y.Y.W)., who has 7 years of experience, independently delineated the lesion areas of hepatocellular carcinoma (HCC) on each image slice using ITK-SNAP software (version 3.8.0, http://www.itksnap.org/), without relying on pathological results or clinical data. A senior radiologist B (H.L., with over 16 years of abdominal imaging experience) then reviewed these delineations and resolved any inconsistencies through consensus. Ultimately, ITK-SNAP software automatically produced the three-dimensional volume of interest (VOI). During the delineation of the region of interest (ROI), particular care was taken to trace the tumor margins accurately, encompassing the tumor capsule while steering clear of blood vessels and bile ducts. Additionally, to assess intraobserver and interobserver consistency in manual segmentation, we randomly chose 40 patients and had their ROIs outlined by the same radiologist A (Y.Y.W.) and radiologist B (H.L.) one month later.

Radiomics features were extracted from the plain, arterial, and venous phase images using the PyRadiomics package (version 2.2.0, https://pyradiomics.readthedocs.io/en/2.2.0/). A standardized preprocessing pipeline was implemented within the PyRadiomics framework, which included isotropic resampling to 1×1×1 mm^3 voxels, intensity normalization, and application of Laplacian of Gaussian (LoG) and Wavelet filters to highlight features at multiple scales. The complete feature extraction parameters, including detailed filter settings and configuration, are comprehensively documented in the Supplementary Material 1. The extracted features included the following classes as defined by PyRadiomics: 1) Shape features, such as surface area, volume, sphericity and so on; 2) First-order gray-level features, representing the energy, entropy, skewness, kurtosis, mean, maximum, and minimum of the ROI voxels; 3) Texture features, including Gray Level Co-occurrence Matrix (GLCM), Gray Level Run Length Matrix (GLRLM), Gray Level Size Zone Matrix (GLSZM), Gray Level Dependence Matrix (GLDM), and Neighboring Gray Tone Difference Matrix (NGTDM).

Feature Selection and Model Building

Before feature selection, all radiomics features underwent Z-score normalization. And the features with interobserver coefficients (ICC) > 0.75 were chosen. To eliminate redundant features, an initial screening of radiomics features was performed using the *T*-test and Mann–Whitney *U*-test ($p < 0.01$). Subsequently, feature selection was performed using the Least Absolute Shrinkage and Selection Operator (LASSO)-logistic regression model. The λ parameter in the LASSO regression was optimized through 10-fold cross-validation, and features with non-zero coefficients were ultimately selected.

After analyzing with the LASSO-logistic model, the dimensionality of features was reduced, and key features were selected from the training cohort. Then, the Rad-score was calculated by adding up the selected radiomics features weighted by their respective coefficients.

Model Performance Assessment

Univariate and multivariate regression analysis were used to determine independent risk clinical and radiological factors of VETC for constructing a clinical model and a radiomics nomogram. And the nomogram incorporating clinical factors, imaging features, and radiomics features was established to create a quantitative predictive tool for VETC. The area under the receiver operating characteristics curve (AUC) was used to evaluate the discrimination among models. Decision curve analysis (DCA) was applied to evaluate the clinical utility of models. Additionally, calibration curves were constructed to assess the predictive accuracy between the actual probability and predicted probability.

Statistical Analysis

The Kolmogorov–Smirnov test was used to determine whether continuous variables followed a normal distribution. Normally distributed variables were presented as mean ± standard deviation (SD), while non-normally distributed variables were presented by median with interquartile range (IQR). Student's *t*-test or the Mann–Whitney *u*-test was applied for continuous variables, and the Pearson χ^2 test or Fisher's exact test was used for categorical variables. Logistic regression analysis, both univariate and multivariate, was performed to identify independent predictors for nomogram construction. Survival curves were generated with the Kaplan-Meier method and compared by a Log rank test.

The "glmnet" software package was utilized for LASSO-logistic regression analysis to select predictive radiomic features. The "rms" and "calibrate" packages were employed to construct the nomogram and calibration curves, respectively. Receiver Operating Characteristic (ROC) curves were plotted, and the AUC was calculated to evaluate the performance of the model. All statistical analyses were performed using R software (version 4.4.2, https://www.r-project.org). A P value < 0.05 was considered statistically significant.

Results

Patients' Characteristics

The baseline clinical and radiological characteristics of all patients are listed in Table 1. The training cohort included 162 patients (58 VETC+ and 104 VETC-), while the validation cohort included 69 patients (19 VETC+ and 50 VETC-). There were no significant differences in the clinical characteristics between the training and validation cohorts (Table 1). The median follow-up time for the entire cohort was 40 months (IQR, 19–48.5 months).

Univariate analysis identified AFP and tumor margin as potential predictors of VETC, while only AFP emerged as an independent risk factor for VETC based on multivariate analysis (p = 0.049). Therefore, AFP was included in the clinical model. The AUC (95% confidence interval [CI]) of the clinical model in the training and validation cohorts was 0.575 (0.501,0.649) and 0.696 (0.569,0.822), respectively.

Radiomics Feature Extraction and Selection

As to the intraobserver and interobserver reproducibility of radiomics feature extraction, the intraobserver ICC of two measurements obtained by radiologist A (Y.Y.W.) were 0.911 (0.806, 0.941); In addition, the interobserver ICCs between radiologist A (Y.Y.W.) and radiologist B (H.L.) were 0.871 (0.759, 0.925), indicating well agreement of manually segmentation and favorable feature extraction reproducibility.

A total of 4851 radiomics features were extracted from CT scans during the plain, arterial and venous phases. After initial screening using the *t*-test and Mann–Whitney *U*-test, 64 radiomics features with $p<0.01$ were selected, and 4 radiomics features were chosen through the LASSO algorithm to calculate the Rad-score (Figure 2). The calculation formula was:

Rad-score Formula = 0.36651 + 0.10996 × lbp_3D_m2_glcm_correlation_V
- 0.08340 × log-sigma-1.0mm-3D_glcm_cluster_shade_A
+ 0.04512 × log-sigma-1.0mm-3D_gldm_large_dependence_ high_gray_level_emphasis_A
+ 0.13230 × square-filter_firstorder_kurtosis_A

Development and Evaluation of a Radiomics Nomogram

In the training cohort, univariate analysis revealed AFP, tumor margin, and Rad-score as significant predictors of VETC (p < 0.05). Multivariate analysis confirmed AFP (OR = 2.04, 95% CI: 0.94–4.43; p = 0.049) and Rad-score (OR = 3.01, 95% CI: 1.91–4.72; p < 0.001) as independent risk factors for VETC (Table 2). A radiomics nomogram integrating AFP and Rad-score was subsequently developed to quantify VETC probability (Figure 3). Calibration curves demonstrated good agreement between observed and predicted probabilities in both cohorts (Figure 4).

The ROC curves indicate that the three predictive models performed reasonably well in identifying VETC (Figure 5). Among these three models, the radiomics nomogram demonstrated the best predictive performance, with an AUC (95% CI) of 0.782 (0.708,0.856) in the training cohort and 0.755 (0.628,0.882) in the validation cohort. DCA demonstrated that

Table 1 Clinical and Radiological Characteristics of HCC Patients in the Training and Validation Cohorts

Characteristics	Training Cohort (n = 162)	Validation Cohort (n = 69)	*P* value
Age (years)*	53.2±10.8	52.3±10.9	0.581
Sex			
Male	22 (13.6)	7 (10.1)	0.614
Female	140 (86.4)	62 (89.9)	
AFP, ng/mL			0.269
< 400	119 (73.5)	45 (65.2)	
≥ 400	43 (26.5)	24 (34.8)	
BMI	22.9 (20.3, 25.4)	23.5 (21.5, 25.8)	0.155
Liver cirrhosis			0.860
No	60 (37.0)	24 (34.8)	
Yes	102 (63.0)	45 (65.2)	
SII	312.8 (230.8, 478.0)	321.6 (208.1, 466.0)	0.597
NLR			1.000
< 2	102 (63.0)	43 (62.3)	
≥ 2	60 (37.0)	26 (37.7)	
PLR			0.585
< 150	140 (86.4)	57 (82.6)	
≥ 150	22 (13.6)	12 (17.4)	
AST, U/L	34.5 (27.0, 45.0)	36.0 (29.0, 50.0)	0.300
ALT, U/L	31.0 (22.2, 45.0)	36.0 (26.0, 49.0)	0.075
Tumor size (cm)	4.1 (2.9, 5.7)	4.7 (3.0, 6.8)	0.167
Intratumoral necrosis			0.621
Present	109 (67.3)	43 (62.3)	
Absent	53 (32.7)	26 (37.7)	
Hepatic vein invasion			0.559
Present	25 (15.4)	8 (11.6)	
Absent	137 (84.6)	61 (88.4)	
Portal vein tumor thrombus			0.837
Present	9 (5.6)	4 (5.8)	
Absent	153 (94.4)	65 (94.2)	
Tumor capsule			0.362
Complete	96 (59.3)	46 (66.7)	
Incomplete/Without	66 (40.7)	23 (33.3)	
Tumor margin			0.067
Smooth	98 (60.5)	47 (68.1)	
Irregular	64 (39.5)	22 (31.9)	

Notes: Data are number of patients; data in parentheses are percentages or median (interquartile range). *Data are means ± standard deviations.

Abbreviations: HCC, hepatocellular carcinoma; AFP, alpha-fetoprotein; BMI, body mass index; SII, systemic immune inflammation index; NLR, neutrophil-to-lymphocyte ratio; PLR, platelet-to-lymphocyte ratio; AST, aspartate aminotransferase; ALT, alanine aminotransferase.

both the radiomics signature and radiomics nomogram provided an overall net benefit superior to the clinical model at the most reasonable threshold probability for predicting VETC in HCC patients (Figure 6).

Survival Prediction

As of November 2024, all patients had completed follow-up. The overall recurrence rate was 51.1% (118/231), with a recurrence rate of 61.0% (47/77) among VETC+ patients and 46.1% (71/154) among VETC- patients. HCC patients with pathologically confirmed VETC+ demonstrated a shorter DFS compared to VETC- HCC patients (HR = 1.59; 95%

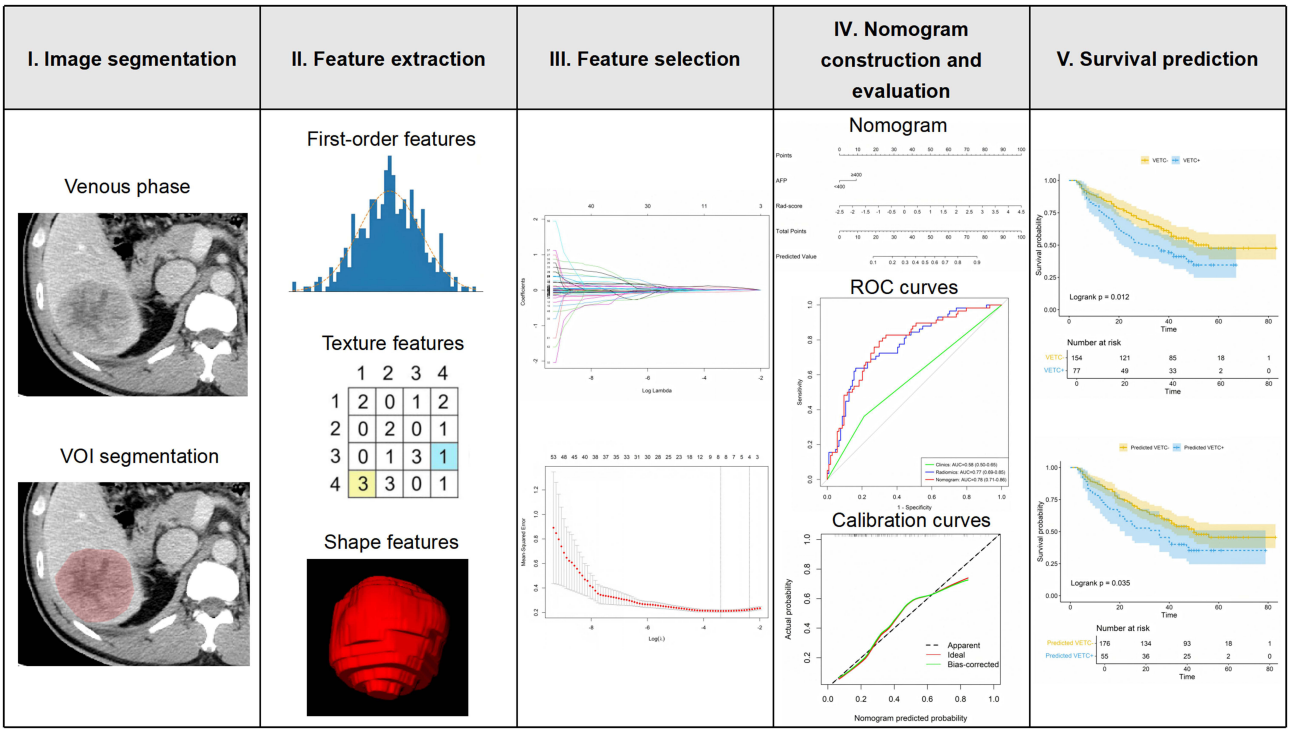

Figure 2 Diagram shows workflow for radiomics image segmentation (**I**), feature extraction (**II**), feature selection (**III**), nomogram construction and evaluation (**IV**), and survival prediction (**V**).

CI: 1.10–2.29; p = 0.012; Figure 7A). Similar prognostic performance was observed in the prediction model, where the DFS of high-risk VETC+ HCC patients predicted by the radiomics nomogram was shorter than that of VETC- HCC patients (HR = 1.55; 95% CI: 1.08–2.23; p = 0.035; Figure 7B).

Table 2 Univariate and Multivariable Logistic Regression Analysis of Predictors of VETC

Characteristics	Univariate Regression Analysis		Multivariate Regression Analysis	
	OR (95% CI)	*p* value	OR (95% CI)	*p* value
Age (years)	1.01 (0.98,1.04)	0.606		
Sex	1.23 (0.47,3.21)	0.675		
AFP	2.12 (1.04,4.32)	0.039	2.04 (0.94,4.43)	0.049
BMI	0.97 (0.88,1.05)	0.427		
Liver cirrhosis	1.34 (0.68,2.62)	0.400		
SII	1.00 (1.00,1.00)	0.657		
NLR	1.19 (0.61,2.31)	0.606		
PLR	1.03 (0.40,2.62)	0.953		
AST	1.00 (0.99,1.02)	0.701		
ALT	1.00 (0.99,1.01)	0.961		
Tumor size (cm)	1.10 (0.94,1.30)	0.241		
Intratumoral necrosis	1.68 (0.81,3.48)	0.166		
Hepatic vein invasion	0.99 (0.41,2.51)	0.911		
Portal vein tumor thrombus	0.73 (0.26–1.99)	0.533		
Tumor capsule	0.93 (0.48,1.79)	0.834		
Tumor margin	1.97 (1.02,3.80)	0.043	1.93 (0.99,3.75)	0.053
Rad-score	3.07 (1.95,4.84)	<0.001	3.01 (1.91,4.72)	<0.001

Abbreviations: VETC, vessels encapsulating tumor clusters; HCC, hepatocellular carcinoma; AFP, alpha-fetoprotein; BMI, body mass index; SII, systemic immune inflammation index; NLR, neutrophil-to-lymphocyte ratio; PLR, platelet-to-lymphocyte ratio; AST, aspartate aminotransferase; ALT, alanine aminotransferase.

https://doi.org/10.2147/JHC.S542092

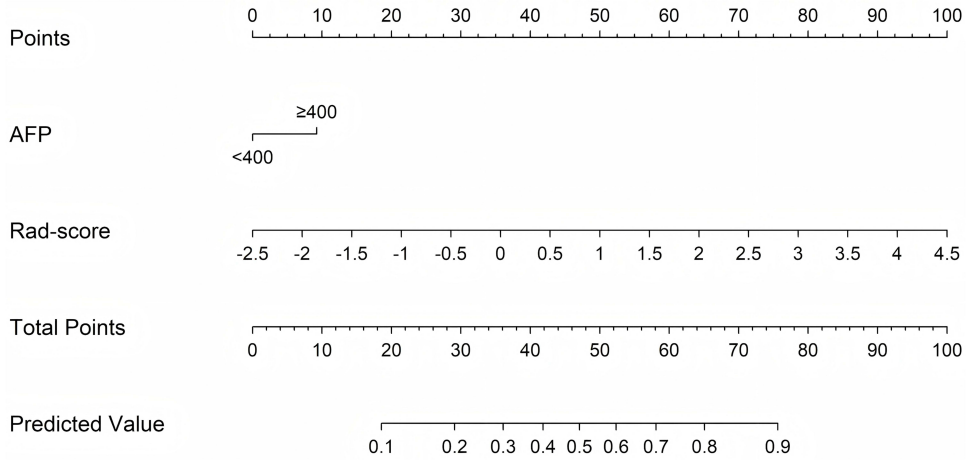

Figure 3 The radiomics nomogram combines clinical factor (AFP) and Rad-score for predicting VETC.
Abbreviations: AFP, alpha-fetoprotein; VETC, vessels encapsulating tumor clusters.

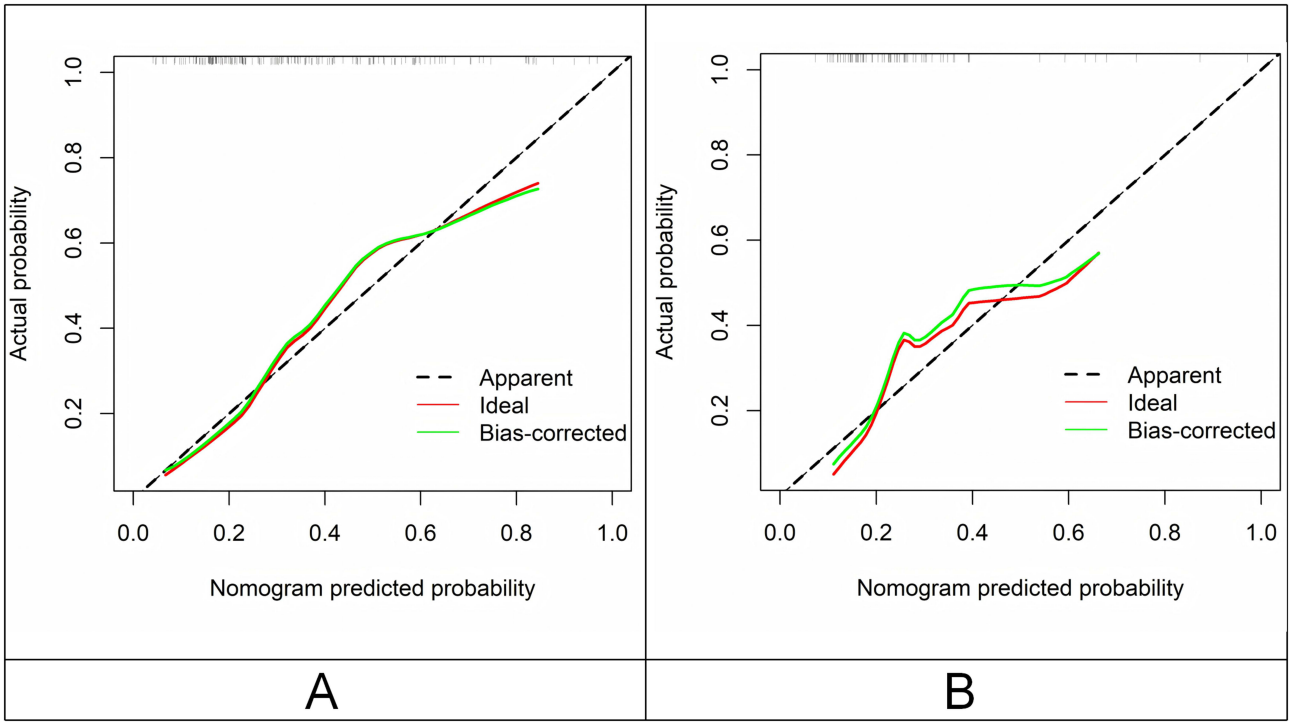

Figure 4 Calibration curves of the radiomics nomogram. (**A**) Training cohort and (**B**) Validation cohort.

Discussion

VETC represents a novel mechanism of vascular metastasis in HCC, strongly linked to a poorer prognosis for patients.[10,11] Currently, VETC assessment relies primarily on histopathological examination after surgery, limiting its clinical applicability. In this study, we developed and validated a non-invasive CT-based radiomics nomogram for predicting VETC in HCC patients preoperatively. This approach integrates AFP with radiomics features. The radiomics nomogram achieved AUCs of 0.782 and 0.755 in the training and validation cohorts, respectively. Additionally, the nomogram correlated with patients' postoperative disease-free survival. This non-invasive prediction method holds promise as a practical preoperative evaluation tool in clinical practice.

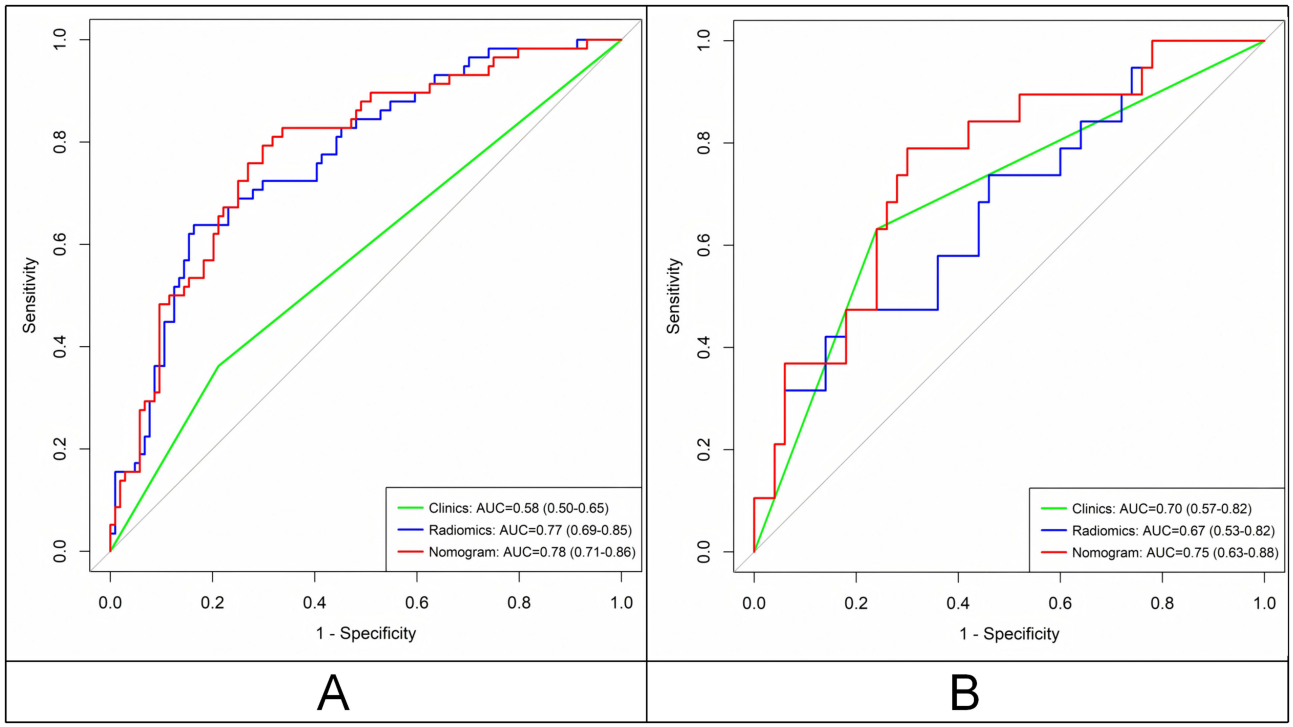

Figure 5 Receiver operating characteristic curves of the clinical model, radiomics signature and radiomics nomogram. (**A**) Training cohort and (**B**) Validation cohort.

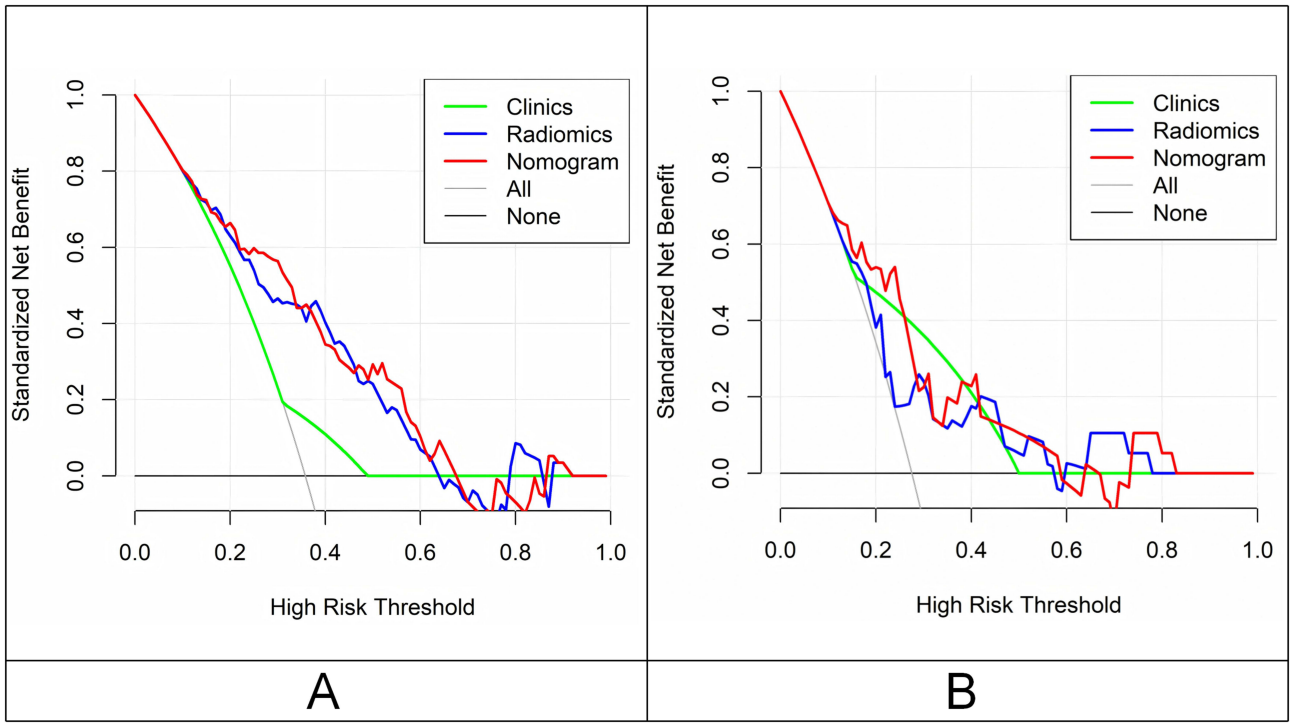

Figure 6 Decision curve analysis for three models. (**A**) Training cohort and (**B**) Validation cohort.

Our study found that AFP is an independent predictor of VETC in the clinical model. Moreover, AFP stands out as the only clinical predictor incorporated into the radiomics nomogram. As the most widely used diagnostic and prognostic serum biomarker for HCC, elevated serum AFP level is strongly associated with poor tumor differentiation and unfavorable clinical outcomes.[19–21] Previous studies have also demonstrated that serum AFP can serve as an independent

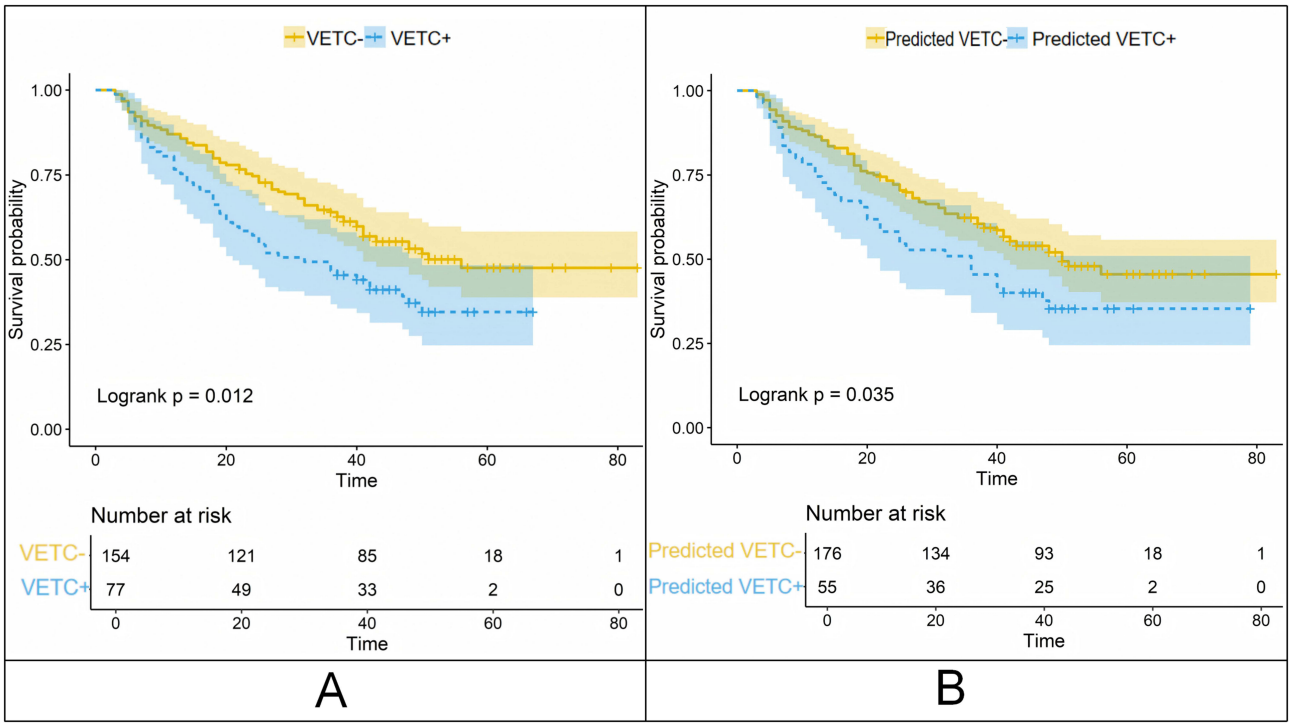

Figure 7 Survival curves according to histological and RN-predicted VETC status. Disease-free survival curves scaled by histologic VETC status (**A**) and RN-predicted VETC status (**B**) with Kaplan-Meier analysis.
Abbreviations: VETC, vessels encapsulating tumor clusters; RN, radiomics nomogram.

predictor of the presence of VETC in HCC.[10,22,23] Additionally, univariate analysis in this study showed a significant correlation between irregular tumor margin and VETC expression. However, this association lost statistical significance in multivariate analysis, potentially due to variable interactions or selection bias in cohort stratification.

With the advancement of computer-aided diagnosis methods, radiomics has been explored for the diagnosis of HCC.[24–26] By quantifying image data, radiomics significantly enhances the objectivity of imaging analysis. While previous studies have established radiomics models based on MRI or ultrasound for predicting VETC in HCC patients with promising results,[27–29] our study focuses on the utility of CT radiomics for this purpose. This approach is motivated by the distinct practical advantages of CT, including its wider availability, lower cost, and faster acquisition times compared to MRI, as well as its greater reproducibility and reduced operator-dependence compared to ultrasound. Consistent with these advantages, our developed CT-based radiomics signature demonstrated higher predictive value for VETC compared to the clinical model. Moreover, the integrated radiomics nomogram, which blends clinical factors with the Rad-score, elevated predictive performance further, highlighting the value of clinical data integration. Additionally, the radiomics nomogram exhibited relatively good and robust performance in both the training and validation cohorts, indicating the potential of CT-based radiomics method for predicting VETC-HCC. Notably, the predictive model developed in this study demonstrated that the key radiomic features were predominantly texture features, showing significantly greater contributions than first-order and shape features. This observation shows consistency with the conclusion of Zhang et al's study based on MRI radiomics for predicting MVI grades, which also identified texture features as major contributors.[30] These results suggest that although vascular invasion patterns (VETC and MVI) differ pathologically, their shared spatial heterogeneity can be effectively characterized through advanced texture analysis. Methodologically, this highlights radiomics' ability to decode tissue microarchitecture, revealing biological heterogeneity in HCC. The biological rationale underlying this link may be that the aberrant microvascular network characteristic of VETC+ HCC causes regional variations in blood flow and intratumoral stroma, which in turn manifest as textural heterogeneity on CT imaging. This proposed mechanism provides a plausible hypothesis for our model's performance that warrants further validation.

Besides, consistent with previous studies, our research also found that histological VETC is associated with poorer HCC prognosis.[10,31] The DFS of VETC+ HCC patients was significantly shorter than that of VETC- HCC patients. Recently, radiomics has been employed by researchers to forecast postoperative prognosis in HCC.[32,33] Both Yu et al[28] and Dong et al[34] reported that the MRI-based radiomics model could be used to preoperatively predict VETC expression and patient prognosis in HCC. Similar findings were observed in our study, indicating that VETC predicted by the radiomics nomogram is an independent predictor of DFS in HCC patients. This provides a convenient and practical auxiliary identification tool for clinical applications. Radiologists can not only utilize this model to analyze patients' preoperative CT images and initially determine the presence of VETC in lesions, but also provide reference opinions for subsequent treatment decisions and assist clinicians in personalized management of patients, such as selecting postoperative adjuvant transcatheter arterial chemoembolization (TACE) and anti-angiogenic targeted drugs.[35,36]

This study has several limitations. First, its retrospective, single-center design is subject to potential selection bias and limits the generalizability of our findings. Second, the manual segmentation of tumors is time-consuming and operator-dependent. Third, the limited number of VETC+ cases in the validation cohort may affect the stability of the performance estimates. Future work should therefore prioritize the development of fully automated segmentation tools to facilitate clinical translation. Finally, external validation in multi-center settings remains essential to conclusively confirm the model's robustness and generalizability.

Conclusion

In conclusion, this study established a non-invasive CT-based radiomics nomogram that integrates AFP and tumor texture features for the preoperative prediction of VETC status in HCC. The model demonstrated favorable performance and effectively stratified patients' postoperative DFS, highlighting its potential as a practical tool for pre-operative risk assessment and personalized therapy planning. Nevertheless, these findings require further validation in large-scale, multicenter, prospective cohorts before they can be adopted into routine clinical practice.

Abbreviations

AFP, alpha-fetoprotein; ALT, alanine transaminase; APHE, arterial phase hyperenhancement; AST, aspartate amino-transferase; AUC, areas under curve; BMI, body mass index; CI, confidence interval; CT, computed tomography; DCA, decision curve analysis; DFS, disease-free survival; FOV, field of view; GLCM, Gray Level Co-occurrence Matrix; GLDM, Gray Level Dependence Matrix; GLRLM, Gray Level Run Length Matrix; GLSZM, Gray Level Size Zone Matrix; HCC, hepatocellular carcinoma; IQR, interquartile range; LASSO, least absolute shrinkage and selection operator; MRI, magnetic resonance imaging; NGTDM, Neighboring Gray Tone Difference Matrix; NRL, neutrophil-to-lymphocyte ratio; PLR, platelet-to-lymphocyte ratio; ROC, receiver operating characteristic; ROI, region of interest; SD, standard deviation; SII, systemic immune inflammation index; TACE, transcatheter arterial chemoembolization; VETC, vessels encapsulating tumor clusters; VOI, volume of interest.

Ethics Approval and Informed Consent

The studies involving human participants were reviewed and approved by the ethics committee of the Guangxi Medical University Cancer Hospital (KYB2023130). The study was completed in accordance with the Declaration of Helsinki, and all patient data are treated confidentially. The requirement for written informed consent was waived by the Institutional Review Board in view of the retrospective observational nature of the research. Before contrast-enhanced abdomen CT and curative hepatic resection, subjects received full information about indications, risks, and alternatives and then signed the written informed consent.

Author Contributions

All authors made a significant contribution to the work reported, whether that is in the conception, study design, execution, acquisition of data, analysis and interpretation, or in all these areas; took part in drafting, revising or critically

reviewing the article; gave final approval of the version to be published; have agreed on the journal to which the article has been submitted; and agree to be accountable for all aspects of the work.

Funding

This work was funded by Guangxi Science and Technology Program (Guike AB23026018), Guangxi Clinical Research Center for Medical Imaging Construction (Guike AD20238096), Guangxi Medical University Youth Science Foundation project (GXMUYSF202335) and Guangxi Natural Science Foundation (2023GXNSFAA026249).

Disclosure

The authors report no conflicts of interest in this work.

References

1. Bray F, Laversanne M, Sung H, et al. Global cancer statistics 2022: GLOBOCAN estimates of incidence and mortality worldwide for 36 cancers in 185 countries. *CA Cancer J Clin*. 2024;74(3):229–263. doi:10.3322/caac.21834
2. Vogel A, Meyer T, Sapisochin G, Salem R, Saborowski A. Hepatocellular carcinoma. *Lancet*. 2022;400(10360):1345–1362. doi:10.1016/S0140-6736(22)01200-4
3. Llovet JM, Kelley RK, Villanueva A, et al. Hepatocellular carcinoma. *Nat Rev Dis Primers*. 2021;7(1):6. doi:10.1038/s41572-020-00240-3
4. Ding T, Xu J, Zhang Y, et al. Endothelium-coated tumor clusters are associated with poor prognosis and micrometastasis of hepatocellular carcinoma after resection. *Cancer*. 2011;117(21):4878–4889. doi:10.1002/cncr.26137
5. Giannelli G, Koudelkova P, Dituri F, Mikulits W. Role of epithelial to mesenchymal transition in hepatocellular carcinoma. *J Hepatol*. 2016;65(4):798–808. doi:10.1016/j.jhep.2016.05.007
6. Aurélie B, Stefano C, Julien C, et al. Gene expression signature as a surrogate marker of microvascular invasion on routine hepatocellular carcinoma biopsies. *J Hepatol*. 2021;76(2):343–352. doi:10.1016/j.jhep.2021.09.034
7. Yunyun W, Wei P, Yunying Q, Danke S, Hai L. Preoperative MR imaging for predicting early recurrence of solitary hepatocellular carcinoma without microvascular invasion. *Eur J Radiol*. 2021;138:109663. doi:10.1016/j.ejrad.2021.109663
8. Wang L, Liang M, Feng B, et al. Microvascular invasion-negative hepatocellular carcinoma: prognostic value of qualitative and quantitative Gd-EOB-DTPA MRI analysis. *Eur J Radiol*. 2023;168:111146. doi:10.1016/j.ejrad.2023.111146
9. Jian-Hong F, Hui-Chao Z, Chong Z, et al. A novel vascular pattern promotes metastasis of hepatocellular carcinoma in an epithelial-mesenchymal transition-independent manner. *Hepatology*. 2015;62(2):452–465. doi:10.1002/hep.27760
10. Salvatore Lorenzo R, Ha Young W, Sarah A, et al. Vessels Encapsulating Tumor Clusters (VETC) Is a powerful predictor of aggressive hepatocellular carcinoma. *Hepatology*. 2020;71(1):183–195. doi:10.1002/hep.30814
11. Zhichao F, Huiling L, Huafei Z, et al. Preoperative CT for characterization of aggressive macrotrabecular-massive subtype and vessels that encapsulate tumor clusters pattern in hepatocellular carcinoma. *Radiology*. 2021;300(1):219–229. doi:10.1148/radiol.2021203614
12. Lu L, Wei W, Huang C, et al. A new horizon in risk stratification of hepatocellular carcinoma by integrating vessels that encapsulate tumor clusters and microvascular invasion. *Hepatol Internat*. 2021;15(3):651–662. doi:10.1007/s12072-021-10183-w
13. Jian-Hong F, Li X, Li-Ru S, et al. Vessels That Encapsulate Tumor Clusters (VETC) pattern is a predictor of sorafenib benefit in patients with hepatocellular carcinoma. *Hepatology*. 2018;70(3):824–839. doi:10.1002/hep.30366
14. Marius EM, Andrzej M, Georg L, et al. Introduction to radiomics. *J Nucl Med*. 2020;61(4):488–495. doi:10.2967/jnumed.118.222893
15. Meng A, Zhuang Y, Huang Q, Tang L, Yang J, Gong P. Development and validation of a cross-modality tensor fusion model using multi-modality MRI radiomics features and clinical radiological characteristics for the prediction of microvascular invasion in hepatocellular carcinoma. *Eur J Surg Oncol*. 2025;51(1):109364. doi:10.1016/j.ejso.2024.109364
16. Masthoff M, Irle M, Kaldewey D, et al. Integrating CT radiomics and clinical features to optimize TACE technique decision-making in hepatocellular carcinoma. *Cancers*. 2025;17(5):893. doi:10.3390/cancers17050893
17. Peng K, Zhang X, Li Z, et al. Myeloid response evaluated by noninvasive CT imaging predicts post-surgical survival and immune checkpoint therapy benefits in patients with hepatocellular carcinoma. *Front Immunol*. 2024;15:1493735. doi:10.3389/fimmu.2024.1493735
18. Lee S, Kim SH, Lee JE, Sinn DH, Park CK. Preoperative gadoxetic acid-enhanced MRI for predicting microvascular invasion in patients with single hepatocellular carcinoma. *J Hepatol*. 2017;67(3):526–534. doi:10.1016/j.jhep.2017.04.024
19. Wei H, Fu F, Jiang H, et al. Development and validation of the OSASH score to predict overall survival of hepatocellular carcinoma after surgical resection: a dual-institutional study. *Eur Radiol*. 2023;33(11):7631–7645. doi:10.1007/s00330-023-09725-7
20. Ridder DA, Weinmann A, Schindeldecker M, et al. Comprehensive clinicopathologic study of alpha fetoprotein-expression in a large cohort of patients with hepatocellular carcinoma. *Int, J, Cancer*. 2022;150(6):1053–1066. doi:10.1002/ijc.33898
21. Yang T, Wei H, Wu Y, et al. Predicting histologic differentiation of solitary hepatocellular carcinoma up to 5 cm on gadoxetate disodium-enhanced MRI. *Insights Imag*. 2023;14(1):3. doi:10.1186/s13244-022-01354-w
22. Pan J, Huang H, Zhang S, et al. Intraindividual comparison of CT and MRI for predicting vessels encapsulating tumor clusters in hepatocellular carcinoma. *Eur Radiol*. 2025;35(1):61–72. doi:10.1007/s00330-024-10944-9
23. Liu Z, Mao Y, Liu L, Li J, Li Q, Zhou Y. Preoperative CT features for characterization of vessels that encapsulate tumor clusters in hepatocellular carcinoma. *Eur. J. Radiol*. 2024;179:111681. doi:10.1016/j.ejrad.2024.111681
24. Mao Y, Wang J, Zhu Y, et al. Gd-EOB-DTPA-enhanced MRI radiomic features for predicting histological grade of hepatocellular carcinoma. *Hepatobil Surg Nutr*. 2022;11(1):13–24. doi:10.21037/hbsn-19-870
25. Lee IC, Huang JY, Chen TC, et al. Evolutionary learning-derived clinical-radiomic models for predicting early recurrence of hepatocellular carcinoma after resection. *Liver Cancer*. 2021;10(6):572–582. doi:10.1159/000518728

26. Liu N, Wu Y, Tao Y, et al. Differentiation of hepatocellular carcinoma from intrahepatic cholangiocarcinoma through MRI radiomics. *Cancers*. 2023;15(22):5373. doi:10.3390/cancers15225373
27. Yang J, Dong X, Wang F, et al. A deep learning model based on MRI for prediction of vessels encapsulating tumour clusters and prognosis in hepatocellular carcinoma. *Abdom Radiol*. 2024;49(4):1074–1083. doi:10.1007/s00261-023-04141-3
28. Yu Y, Fan Y, Wang X, et al. Gd-EOB-DTPA-enhanced MRI radiomics to predict vessels encapsulating tumor clusters (VETC) and patient prognosis in hepatocellular carcinoma. *Eur Radiol*. 2022;32(2):959–970. doi:10.1007/s00330-021-08250-9
29. Xu W, Zhang H, Zhang R, et al. Deep learning model based on contrast-enhanced ultrasound for predicting vessels encapsulating tumor clusters in hepatocellular carcinoma. *Eur Radiol*. 2025;35(2):989–1000. doi:10.1007/s00330-024-10985-0
30. Zhao Z, Xiu-Fen J, Xiao-Yu C, Yong-Hua C, Ke-Hua P. Radiomics-based prediction of microvascular invasion grade in nodular hepatocellular carcinoma using contrast-enhanced magnetic resonance imaging. *J Hepatocell Carcinoma*. 2024;11:15–27. doi:10.2147/jhc.S461420
31. Zhang P, Ono A, Fujii Y, et al. The presence of vessels encapsulating tumor clusters is associated with an immunosuppressive tumor microenvironment in hepatocellular carcinoma. *Int J Cancer*. 2022;151(12):2278–2290. doi:10.1002/ijc.34247
32. Xu X, Zhang HL, Liu QP, et al. Radiomic analysis of contrast-enhanced CT predicts microvascular invasion and outcome in hepatocellular carcinoma. *J Hepatol*. 2019;70(6):1133–1144. doi:10.1016/j.jhep.2019.02.023
33. Kim S, Shin J, Kim DY, Choi GH, Kim MJ, Choi JY. Radiomics on gadoxetic acid-enhanced magnetic resonance imaging for prediction of postoperative early and late recurrence of single hepatocellular carcinoma. *Clin Cancer Res*. 2019;25(13):3847–3855. doi:10.1158/1078-0432.CCR-18-2861
34. Dong X, Yang J, Zhang B, et al. Deep learning radiomics model of dynamic contrast-enhanced mri for evaluating vessels encapsulating tumor clusters and prognosis in hepatocellular carcinoma. *J Magn Reson Imaging*. 2024;59(1):108–119. doi:10.1002/jmri.28745
35. Wang J, Li X, Tang H, et al. Vessels that encapsulate tumor clusters (VETC) pattern predicts the efficacy of adjuvant TACE in hepatocellular carcinoma. *J Cancer Res Clin Oncol*. 2023;149(8):4163–4172. doi:10.1007/s00432-022-04323-4
36. Pan J, Zhang C, Huang H, et al. Deciphering the prognostic and therapeutic value of a gene model associated with two aggressive hepatocellular carcinoma phenotypes using machine learning. *J Hepatocell Carcinoma*. 2024;11:2373–2390. doi:10.2147/JHC.S480358